



## Nickel Peroxide Nanoparticles as an Efficient Catalyst for Nitrile Hydration: Synthesis, Characterization, and Mechanistic Insights

Abdulraheem S.A. Almalki

Department of Chemistry, Faculty of Science, Taif University, Taif, 21974 Saudi Arabia

Received: 01 Mar. 2025

Accepted: 20 Mar. 2025

Published: 30 Mar. 2025

### ABSTRACT

The catalytic systems  $\text{NiCl}_2 \cdot 6\text{H}_2\text{O}$ ,  $\text{CuCl}_2 \cdot 6\text{H}_2\text{O}$ , and  $\text{Fe}(\text{NO}_3)_3 \cdot 9\text{H}_2\text{O}/\text{NaOH}/\text{NaOCl}$  (pH, 13) were investigated for the catalytic hydration of ten nitriles to their corresponding amides at room temperature. Benzonitrile was used as a model substrate to optimize reaction conditions, and nine additional substrates were selected to explore the reaction's scope. The resulting amides were obtained in moderate to high yields. Various parameters, such as yield (Y%), turnover (TO), and turnover frequency (TOF), were calculated to identify the most effective metal salt for maximizing amide yields. It was found that the  $\text{NiCl}_2 \cdot 6\text{H}_2\text{O}/\text{NaOH}/\text{NaOCl}$  catalytic system exhibited the best catalytic performance, with a TOF of  $15.8 \text{ h}^{-1}$ . Consequently, the active species responsible for nitrile hydration was isolated and characterized as nickel peroxide nanoparticles, which were generated in situ. Characterization techniques included X-ray powder diffraction (XRD), Fourier transform infrared spectroscopy (FTIR), scanning electron microscopy (SEM), transmission electron microscopy (TEM), and zeta potential measurements. SEM and TEM images of the nickel peroxide samples revealed fine spherical-like aggregates of  $\text{NiO}_2$  molecules with a nearly uniform particle size, ranging from 2 to 3 nm. The proposed mechanism involves the reaction of  $\text{NiCl}_2 \cdot 6\text{H}_2\text{O}$  with  $\text{NaOCl}$  to produce  $\text{NiO}_2$  nanoparticles, which then react with the nitrile substrate to form the corresponding amides and  $\text{NiO}$ . The reaction continues until the substrate is fully consumed. The resulting  $\text{NiO}$  is recycled with excess  $\text{NaOCl}$  for further catalytic hydration reactions.

**Keywords:** Catalytic, Nitriles, Amides,  $\text{NaOCl}$ , Hydration.

### 1. Introduction

Amides are a vital organic compounds containing carbonyl group ( $\text{C}=\text{O}$ ) bonded to a nitrogen atom (N). Their significance spans various fields, including pharmaceuticals, agriculture, and materials science. Amides are important organic compounds, found in proteins, agrochemicals, pharmaceutical and natural products. In the pharmaceutical industry, the formation of amides is among the most frequently employed reactions. Around 25% of all synthesized drugs contain at least one amide bond (Montalbetti and Falque, 2005 and de Figueiredo *et al.*, 2016). These bonds are present in widely used over-the-counter medications, such as ibuprofen and melatonin, as well as in prescription antibiotics like penicillin and amoxicillin. In agriculture, amide-based herbicides are widely used globally to manage unwanted plant growth and enhance crop yields (Hu *et al.*, 2008). In materials science, several materials were synthesized including polymers (Han and Wu, 2022), electrolytes (Wu *et al.*, 2022), and biomodifiers (Kabirb *et al.*, 2021). The amide bond formation from nitriles is one of the most important transformations in synthetic chemistry (Pattabiraman and Bode 2011, Feng *et al.*, 2022). In the light of our interests to the organic synthesis by transition metal complexes (Feng *et al.*, 2022; Alsharif *et al.*, 2022; Ali *et al.*, 2021 and Almalki *et al.*, 2022) we decided to study the hydration of some nitriles to amides. Different techniques were used but were expensive, toxic and resulted an environmental impact of waste streams (Massolo *et al.*, 2020). Thus, the development of more efficient, greener and catalytic protocols is still a great demand in synthetic chemistry. Recently, the synthesis of amides was reported

**Corresponding Author:** Abdulraheem S.A. Almalki, Department of Chemistry, Faculty of Science, Taif University, Taif, 21974 Saudi Arabia. E-mail: drasaalmalki1@gmail.com

by oxidative cleavage of 1,2-dioils using  $\text{NH}_4\text{OAC}$  as source of nitrogen (Luo *et al.*, 2023). Duan, and Song, (2024) reported the nickel catalyzed photoredox carbamidation of oxamic with a series of (hetero) arylhalides to the corresponding amides. Nickel and manganese were dispersed in alumina and the powders were used for catalytic hydration of nitriles to amides (Govindaraj *et al.*, 2024). The most comment route for the synthesis of amides is the Beckmann rearrangement, Borah reported the synthesis of some amides from their corresponding aldoximes using  $\text{Fe}_3\text{O}_4\text{-Pd@rGO NC}$  as a catalyst (Hazarika and

Hazarika and Borah, (2023). Amides were made via an anodic electrocatalytic coupling of alcohol and ammonia, in this reaction the  $\beta\text{-Ni(OH)}_2$  catalyst was grown on the Ni foam to acquire higher apparent activity ( Lu *et al.*, 2024). Iron and cobalt complexes were prepared and characterized and used for amides synthesis by couplinf alcohol and amines (Almada, 2023). Several amides were synthesized by refluxing aryl halides with nitroarenes by using  $\text{NiCl}_2(\text{glyme})$  as a catalyst ( Cheung *et al.*, 2018). Nickel peroxide ( $\text{NiO}_2$ ) is an inorganic compound that exhibits unique properties, making it valuable in various applications. Nickel peroxide had been used as a catalyst for the synthesis of many organic compounds, of which oxidation of alcohols (Nakagawa *et al.*, 1962), synthesis of benzoxazoles from Schiff's bases (Nakagawa *et al.*, 1964), oxidation of amines (Nakagawa and Tsuji, 1963), oxidation of canthaxanthin ( Lutz-Röder *et al.*, 1999), Synthesis of nitriles from aldehydes (Nakagawa *et al.*, 1979), synthesis of amides from aldehydes or alcohols (Nakagawa *et al.*, 1966) have been reported. As a transition metal oxide,  $\text{NiO}_2$  is recognized for its catalytic activity, particularly in oxidation reactions, where it facilitates the conversion of organic compounds (Sreenavya *et al.*, 2021; Dey and Mehta, 2020 and Ogoshi 2020). Its ability to exist in different oxidation states allows for versatile interactions with various substrates, enhancing its role in catalysis and electrochemistry. In addition to its catalytic applications,  $\text{NiO}_2$  has garnered interest in the field of materials science, particularly for its potential use in batteries, fuel cells, and sensors ( Ambalgi *et al.*, 2016 and Aziz, 2020). The compound's nanostructured forms, such as nanoparticles, demonstrate improved surface area and reactivity, further enhancing its performance in these applications ( Moradnia *et al.*, 2024 and Singh *et al.*, 2019). Shoaib *et al.* (2023) examined the catalytic dehydrogenation of benzylamine and various para-substituents to their corresponding nitriles using the nanostructured  $\text{NiO}_2$  (prepared in situ from the catalytic system  $\text{NiSO}_4 \cdot 6\text{H}_2\text{O}/\text{NaOCl}$ ) in an aqueous basic medium. Conventional nitrile hydration for amide synthesis typically requires strong acids or bases. In strong base conditions, cyano groups tend to over-hydrolyze into acids, and the resulting amides can further react to form salts, complicating product separation (Ahmed *et al.*, 2011). While strong acids can control hydrolysis at the amide stage, the reaction requires pre-cise control of temperature and the nitrile-to-water ratio. To address the limitations of traditional acid/base catalysis, researchers have developed various homogeneous and heterogeneous catalytic systems for nitrile hydration, Table 1 exposes some reported data related to nitrile hydration.

Here we report a simple and expensive protocol for hydration of nitriles to amides in an aqueous basic medium at room temperature using the catalytic system  $\text{NiCl}_2 \cdot 6\text{H}_2\text{O} / \text{NaOCl}/\text{NaOH}$ . The active species was isolated, characterized and a plausible mechanism was suggested.

**Table 1:** Catalytic systems for nitrile hydration

Catalytic system	Temperature (°C)	Reference
$[\text{Ru}(\text{H}_2\text{O})(\text{NCMe})_4(\text{PiPr}_3)]\text{BF}_4$	55	Martin <i>et al.</i> (2009)
$\text{RuCl}_3 \cdot n\text{H}_2\text{O}$	76	Cariati <i>et al.</i> (2003)
$\text{OsCl}_3 \cdot n\text{H}_2\text{O}$	76	Djoman and Ajjou (2000)
$[\text{Rh}(\text{COD})\text{Cl}]_2$	80	Kaminskaia <i>et al.</i> (1998)
$[(\text{dippe})\text{Ni}(2\text{-NCCH}_3)]$	180	Martin <i>et al.</i> (2009)
$\text{K}_2\text{PdCl}_4$ , 2,2-bipy, NaOH	76	[Kopylovich <i>et al.</i> (2002)
$\text{Zn}(\text{NO}_3)_2 \cdot 6\text{H}_2\text{O}/2\text{-propanone oxime}$	76	Tilvez <i>et al.</i> (2013)
$[\text{Pd}(\text{OH})_4]^{2+}$	76	Wang <i>et al.</i> (2019)
(NR- $\text{MnO}_2$ )	76	Vyas <i>et al.</i> (2020)
Arene-ruthenium(II) complexes	80	Waqas <i>et al.</i> (2020)

## 2. Materials and methods

### 2.1 Materials

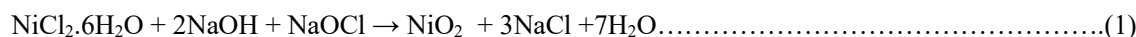
All chemicals  $\text{NiCl}_2 \cdot 6\text{H}_2\text{O}$ ,  $\text{CuCl}_2 \cdot 6\text{H}_2\text{O}$ ,  $\text{Fe}(\text{NO}_3)_3 \cdot 9\text{H}_2\text{O}$ , benzonitrile (BzCN), and *p*-substituted benzonitrile R-BzCN (R =  $\text{CH}_3$ , OH,  $\text{NH}_2$ , CN,  $\text{NO}_2$ , and  $\text{F}_3\text{C}$ ), furan-2-carboxnitrile, pyridine-3-carbonitrile and quoline-2-carbonitrile were used without purification and purchased from Sigma-Aldrich (Germany, Berlin) and NaOCl was purchased from local market and the concentration was determined by iodometric technique (van der Waal, 2014).

### 2.2 Synthesis of $\text{NiO}_2$

A modified procedure for synthesis of  $\text{NiO}_2$ . To a 10 mL of one molar NaOH,  $\text{NiCl}_2 \cdot \text{H}_2\text{O}$  (260 mg, 2 mmol) was added with stirring. NaOCl (20 mL, 5.5%) was added dropwise within two 2 hours. The fine black microcrystals were collected by filtration, washed thoroughly with deionized water, and dried at  $60^\circ\text{C}$  for 14 hours.

### 2.3 Catalytic hydration of nitriles to amides

To a 50 ml round-bottom flask equipped in ice-bath and magnetic stirrer were added metal salt hexahydrate (0.2 mmol), 10 ml NaOH (1.0 molar) and nitrile (10 mmol), The cooled NaOCl (20 mL, 5.25%, 100 mmol) was added dropwise within one hour and the reaction mixture was further stirred for two hours until the fine black  $\text{NiO}_2$  is completely disappeared. The produced amide with then extracted, dried, and characterized by GC-MS.



### 2.4 Recycling of NiO

The NiO that produced after work-up of the catalytic hydration reaction was washed with acetone and water to remove the impurities. The solid was treated again with a molar NaOH and NaOCl (ten fold excess of the solid) to provide  $\text{NiO}_2$  which was washed and dried.



### 2.5 Characterization

The X-ray diffraction for phase identification was conducted using a JSX-60PA/Jeol diffractometer from Japan with Ni-filtered  $\text{CuK}\alpha$  radiation ( $\lambda=1.5418 \text{ \AA}$ ). Scanning electron microscopy (SEM) was performed with an FEGSEM, THERMOSCIENTIFIC QUATTRO S. Transmission electron microscopy (TEM) analysis utilized a JEM 100 CXII TEM operating at 80 kV. Fourier-transform infrared spectroscopy (FTIR) spectrum was captured using an Alpha-Bruker FTIR spectrophotometer (model no. 200695, Berlin, Germany). Thermogravimetric analysis (TGA) was conducted in static air over the temperature range of  $25^\circ\text{C}$  to  $900^\circ\text{C}$  at a heating rate of  $10.0^\circ\text{C}/\text{min}$  using the TGA Q50 V20.13 Build 39 thermogravimetric analyzer. The Brunauer–Emmett–Teller (BET) analysis was conducted using St 2 on the NOVA touch 4LX analyzer from Quantachrome Instruments and the sample was evacuated at  $150^\circ\text{C}$  for two hours under a flow of  $\text{N}_2$ . Subsequently, this sample was analyzed with liquid nitrogen to obtain full adsorption-desorption isotherm, and then surface area and porosity were calculated. Zeta potential measurement of the prepared nickel peroxide was conducted using the Zetasizer Ver. 8.02 (Malvern Instruments Ltd, England).

## 3. Results and Discussion

### 3.1 Characterization of $\text{NiO}_2$ nanoparticles

Fig. 1 (a and b) exposes the SEM and TEM images of the prepared sample. The morphology of the nanocrystallites as depicted in Fig. 1(a) indicates a high degree of agglomeration among the particles forming polyhedral or faceted structures. Their surface texture indicates a crystalline nature with distinct grain boundaries. Based on the 500 nm scale bar, individual particles appear to range in size from approximately 50 to 200 nm. Bright contrast areas in the image may signify surface roughness or the presence of secondary phase formations. Additionally, small white particles or clusters could represent residual precursors, byproducts, or unreacted materials. The nanoparticles are densely packed, suggesting potential sintering or further aggregation, which could impact their catalytic activity and

surface area.. The Transmission Electron Microscopy (TEM) image displays the spherical nanoparticles prepared, as illustrated in Fig. 1(b). Alongside individual particles, there are also aggregated particles present. The X-ray diffraction patterns of the NiO<sub>2</sub> nanoparticle samples are displayed in Fig. 2. This Figure reveals major diffraction peaks at 37.68°, 39.05°, 43.92°, 64.30°, and 77.41°, corresponding to the (101), (012), (009), (110), and (012) crystallographic directions, re-spectively, characteristic for NiO<sub>2</sub> (JCPDS no. 01-085-1977) (Wei *et al.*, 2009). The average crystallite size of NiO<sub>2</sub> was calculated using the Debye-Scherrer equation: (Qiao *et al.*, 2009).

$$D = \frac{K \lambda}{\beta \cos \theta}$$

Where D represents the average crystallite size,  $\lambda = 1.54056 \text{ \AA}$  is the wavelength of CuK $\alpha$  radiation,  $\beta$  denotes the full width at half-maximum (FWHM) intensity of the peak in radians,  $\theta$  stands for Bragg's diffraction angle, and K is a constant typically set to 0.9. The calculated crystallite size (using the Scherrer relation) is 45, 38, 41, and 38 nm for the four patterns, respectively (with an average of 40 nm), validating the presence of a nano-crystalline structure consistent with the TEM analyses.

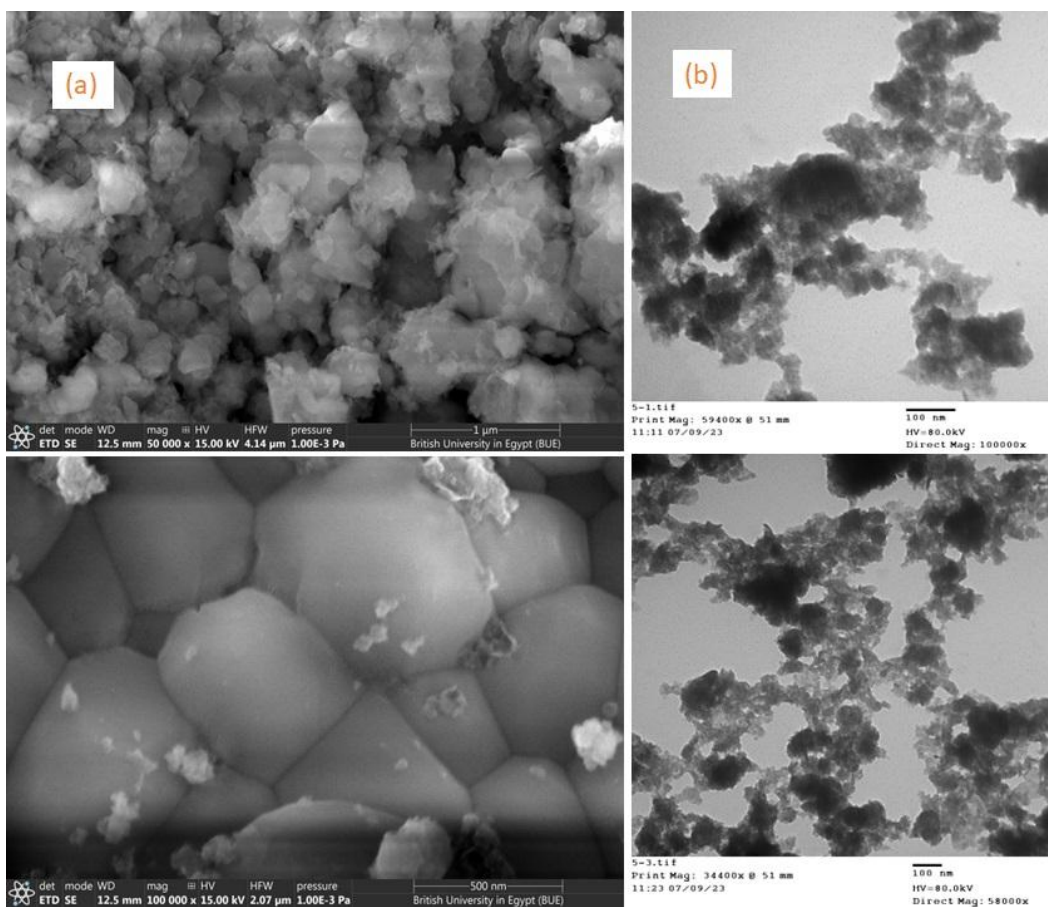


Fig. 1: SEM (a) and TEM image (b) for the prepared NiO<sub>2</sub> nanoparticles.

Fig. 3 illustrates the FTIR spectrum of NiO<sub>2</sub> nanoparticles, displaying several notable absorption bands. The two absorption bands appeared at 590 and 680 cm<sup>-1</sup> corresponds to the Ni-O and Ni-O-H stretching vibration mode, respectively ( Yang *et al.*, 2007 and Cheng *et al.*, 2010). The use of smaller-sized samples in this study compared to bulk NiO<sub>2</sub> resulted in a blue shift in the IR band of Ni-O stretching vibration for NiO<sub>2</sub> nanoparticles. This blue shift is attributed to the quantum size effect and the spherical nanostructures of the NiO<sub>2</sub> nanoparticles, distinguishing their FTIR absorption from that of the bulk form (Qiao *et al.*, 2009). Additionally, the broad absorption peak centered at 3400 cm<sup>-1</sup> is

linked to O–H stretching vibrations, while the weak band near  $1640\text{ cm}^{-1}$  is associated with H–O–H bending vibrations, potentially induced by water adsorption during sample preparation. These observations indicate the influence of hydration on the structure and suggest the presence of hydroxyl groups in the precursor material. The absorption band appeared at  $1105\text{ cm}^{-1}$  is attributed to O–C=O symmetric and asymmetric stretching vibrations, as well as C–O stretching vibration. The presence of carbon in the metal oxide is attributed to contaminations through preparation process.

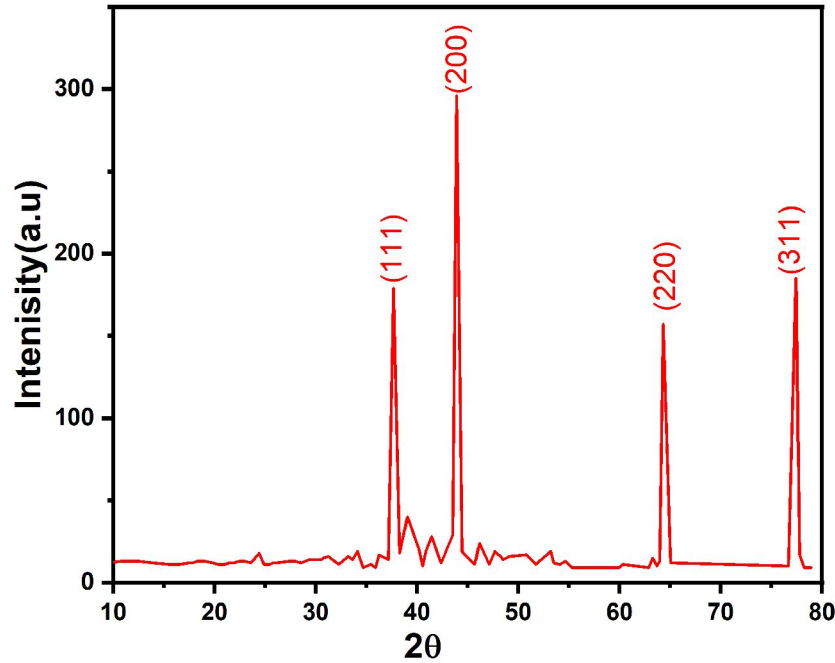


Fig. 2: XRD patterns for the prepared NiO<sub>2</sub> nanoparticles.

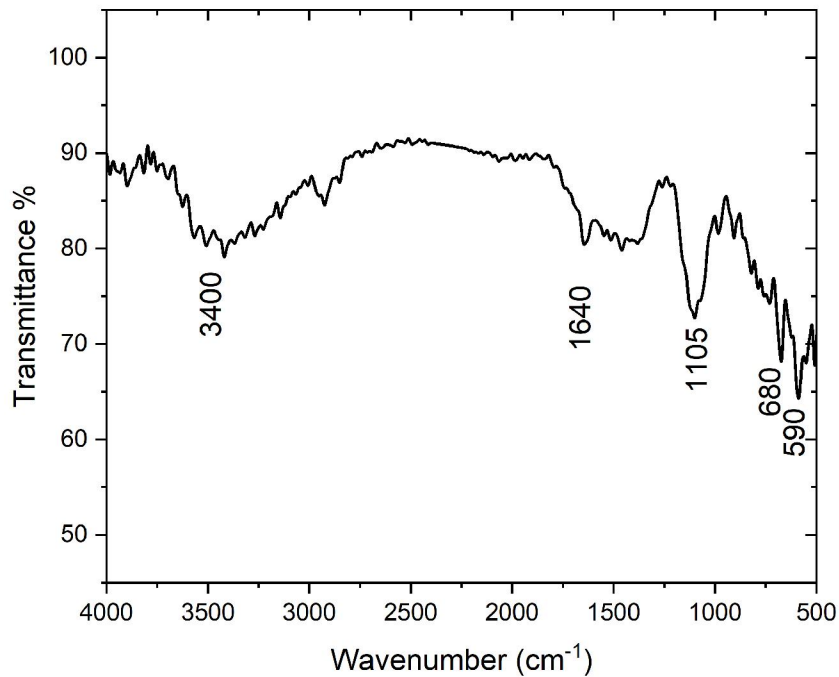


Fig. 3: FTIR spectrum for the prepared NiO<sub>2</sub> nanoparticles.

The N<sub>2</sub> adsorption-desorption isotherm was examined using the BET method to determine the specific surface area and porosity of the sample. Fig 4(a and b) displays the N<sub>2</sub> sorption isotherm and

pore size distribution. The N<sub>2</sub> adsorption isotherm was utilized to assess the BET surface area and pore volume. According to the IUPAC, the N<sub>2</sub> sorption isotherm of NiO<sub>2</sub> can be classified as type IV with H3 hysteresis loop, characteristic for mesoporous material (Cychosz *et al.*, 2017), which agree with the data of pore size distribution (Fig. 4b). The C<sub>BET</sub> constant 8.3, Surface area (S<sub>BET</sub>) 38.6 m<sup>2</sup>/g, average pore radius 2.77 nm, pore volume 0.044 cc/g, total pore volume 0.053 cc/g for pores smaller than 161.42 nm (radius) at relative pressure 0.99402. Fig.5 showed the zeta potential of prepared sample powder and found to be negative charge (-3.98 mV). The zeta potential is a measure of the electrical charge at the slipping plane of a particle. When the zeta potential is equal to -3.98 mV, it indicates that the particles possess a negative surface charge. The magnitude of the zeta potential (-3.98 mV in this case) suggests the strength of the repulsive or attractive forces between particles. A negative zeta potential typically indicates that the particles will repel each other, which can affect the stability and behavior of the system.

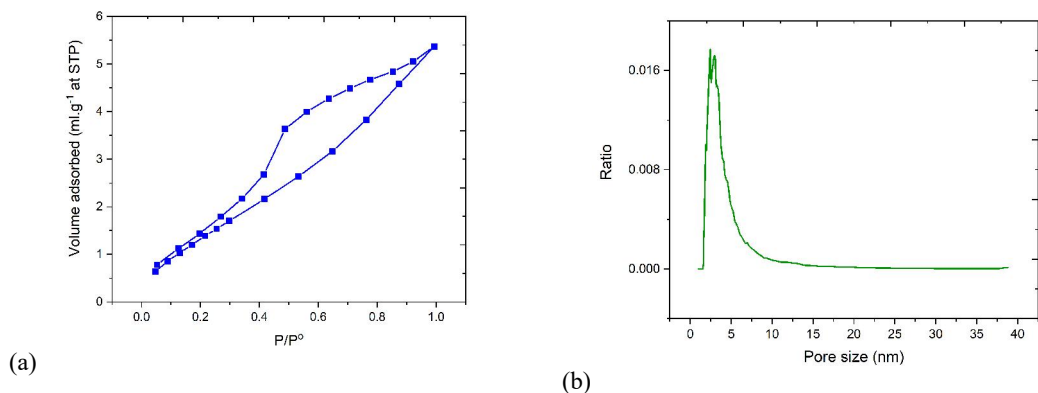


Fig. 4: N<sub>2</sub> sorption isotherm (a) and pore size distribution (b).

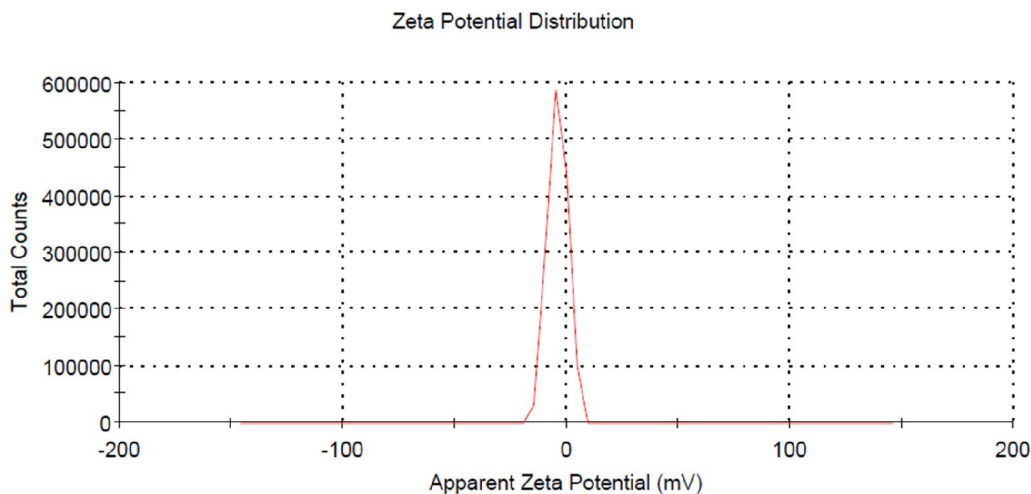


Fig. 5: Zeta potential of NiO<sub>2</sub>

The thermal events of NiO<sub>2</sub>, shown in Fig 6. From Fig. 6, continuous mass loss is observed up to 500 °C, after which the mass stabilizes with further heating. Moreover, three significant mass losses of 6.9%, 5.2%, and 6.9% were noted between approximately 57–204 °C, 204–257 °C, and 257–419 °C, respectively. The first peak corresponds to the evaporation of water (Arai *et al.*, 2002), the second peak around 257 °C indicates the oxidation of the precursor to form NiO, and the third peak at 370 °C is attributed to the formation of oxygen vacancies in the synthesized nanoparticles (Rehman *et al.*, 2023). The thermal events of the prepared sample indicated that it has high thermal stability.

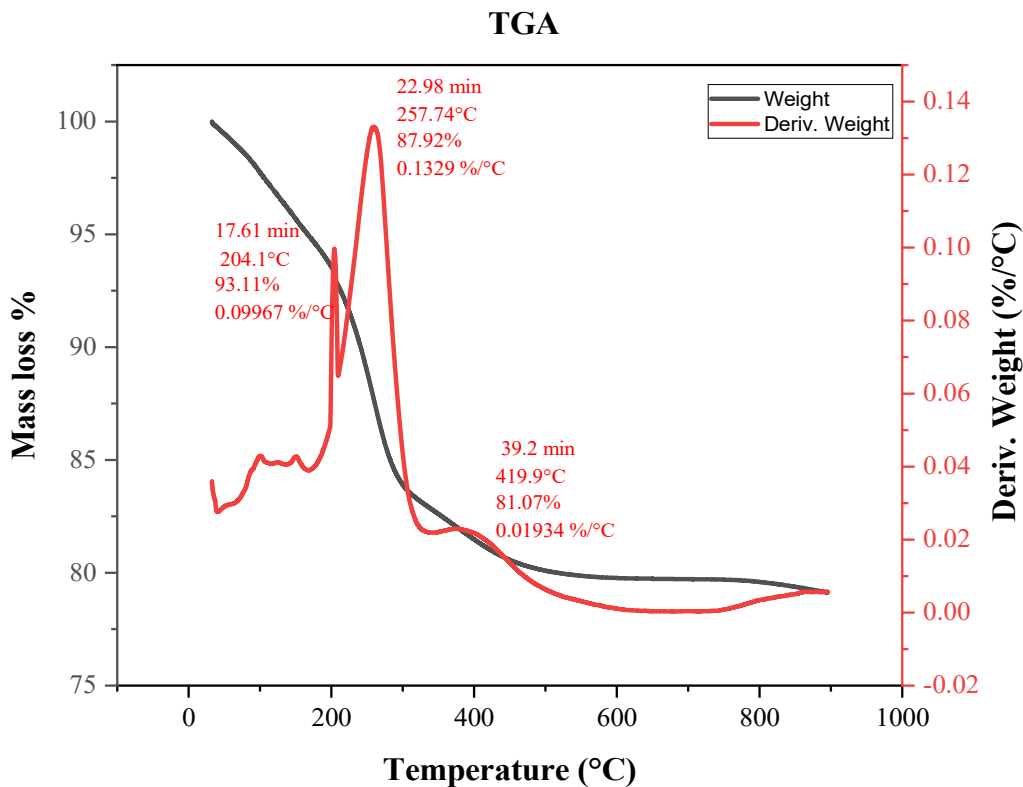
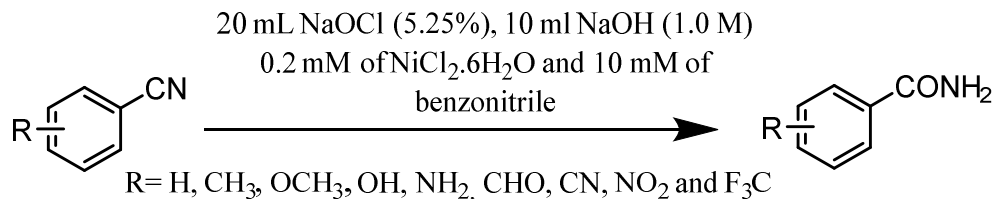


Fig. 6: Thermal events, TGA, of the prepared NiO<sub>2</sub> sample.

### 3.2. Catalytic conversions of nitriles to amides

The catalytic conversion of ten nitriles to their corresponding amides by the catalytic systems, NiCl<sub>2</sub>·6H<sub>2</sub>O, CuCl<sub>2</sub>·6H<sub>2</sub>O and Fe(NO<sub>3</sub>)<sub>3</sub>·9H<sub>2</sub>O/NaOH/NaOCl (pH= 13) at room temperature has been investigated. Different reaction conditions were performed to discover the best inexpensive, selective, and highly yielded protocol for hydration of these nitriles to their amides.



Scheme 1. Catalytic hydration of benzonitrile and some *p*-substituted benzonitrile by NiCl<sub>2</sub>·6H<sub>2</sub>O (0.2 mM), CuCl<sub>2</sub>·6H<sub>2</sub>O (0.2 mM) and Fe(NO<sub>3</sub>)<sub>2</sub>·9H<sub>2</sub>O /NaOH/NaOCl.

A number of experiments were performed in which, benzonitrile was selected as a model substrate with NiCl<sub>2</sub>·6H<sub>2</sub>O (0.2 mM), CuCl<sub>2</sub>·6H<sub>2</sub>O (0.2 mM) and Fe(NO<sub>3</sub>)<sub>2</sub>·6H<sub>2</sub>O (0.2 mM) as metal salts and in the presence of NaOCl (20 mL, 5.25%, 100 mM) as an inexpensive co-oxidant to find the best conditions for hydration of benzonitrile to benzamide. The scope of these catalytic systems was also studied using different substrates. All results were summarized in Table 2.

It was noticed the catalytic system, NiCl<sub>2</sub>·6H<sub>2</sub>O (0.2 mM)/NaOH (10 ml of a molar and NaOCl (20 mL, 5.25%; 100-fold-excess of the substrate))/NaOH (10 mL, 1.0 M) catalyzed the conversion benzonitrile (10 mM) to benzamide at room temperature in 95% yield by stirring the reaction mixture for three hours. Replacement of NiCl<sub>2</sub>·6H<sub>2</sub>O by CuCl<sub>2</sub>·6H<sub>2</sub>O (0.2 mM) and Fe(NO<sub>3</sub>)<sub>2</sub>·9H<sub>2</sub>O under the

same conditions gave 72% and 60% yields respectively. The low yields in these two experiments are probably due the low solubility of these metal salts under these reaction conditions or low activities of the formed active species (entry 1, Table 2) (Waqas *et al.*, 2020). Since the efficiency of the catalyst can be measured by calculating the turnover frequency (TOF) which is equal to the number of moles of product formed per mole of catalyst per unit time, we calculated, the yields (Y%), turnover (TO) and turn over frequency (TOF) according to equations 1-3 (Chowdhury *et al.*, 2022; Kozuch and Martin, 2012 and Comotti *et al.*, 2004).

$$\text{Yield (Y\%)} = \frac{\text{Moles of amide}}{\text{Moles of nitrile}} \dots\dots\dots(3)$$

$$\text{Turn over (TO)} = \frac{\text{Moles of amide}}{\text{Moles of catalyst}} \dots\dots\dots(4)$$

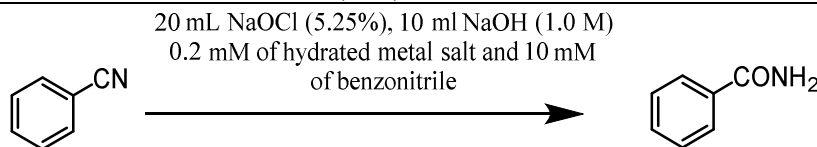
$$\text{Turn over (TO)} = \frac{\text{Turnover}}{\text{Time (h)}} \dots\dots\dots(5)$$

Attempts to hydrate benzonitrile to benzamide without addition of these salts were all unsuccessful since benzamide was not detected (entry 2, Table 2).

Three experiments were conducted at 60°C, 80 °C and 100 °C respectively (entry 3, 4 and 5 Table 2), the yields of benzamide were 40%, 30% at 60°C, 80 °C respectively, while at 100 °C, benzamide was not detected. This is probably due to the fact that the shelf-time of NaOCl is small and decomposed upon increasing temperature (Sirtes *et al.*, 2005).

**Table 2:** Optimum conditions for catalytic hydration of benzonitrile (BzCN) to benzamide (BzCONH<sub>2</sub>) by NiCl<sub>2</sub>.6H<sub>2</sub>O, CuCl<sub>2</sub>.6H<sub>2</sub>O and Fe(NO<sub>3</sub>)<sub>3</sub>.9H<sub>2</sub>O / NaOCl/NaOH.

Entry	NiCl <sub>2</sub> .6H <sub>2</sub> O			CuCl <sub>2</sub> .6H <sub>2</sub> O			Fe(NO <sub>3</sub> ) <sub>3</sub> .6H <sub>2</sub> O		
	Y (%)	TO	TOF (h <sup>-1</sup> )	Y (%)	TO	TOF (h <sup>-1</sup> )	Y (%)	TO	TOF (h <sup>-1</sup> )
1	95	47.5	15.8	72	36	12	60	30	7.5
2	0	0	0	0	0	0	0	0	0
3	40	20	6.7	25	12.5	4.2	10	5	1.7
4	30	15	5	20	10	3.3	8	4	1.3
5	0	0	0	0	0	0	0	0	0
<b>Entry</b>	<b>Y(%)</b>			<b>TO</b>			<b>TOF (h<sup>-1</sup>)</b>		
6	60			30			7.7		
7	50			25			8.3		
8	43			21.5			7.2		



The produced grey green nickel oxide powder (NiO) was isolated by filtration, filtered and washed with deionized water and acetone to remove impurities then dried. The produced NiO was recycled and used instead of NiCl<sub>2</sub>.6H<sub>2</sub>O three times (entries; 6,7 and 8 Table 2) for further catalytic conversions of benzonitrile to the corresponding benzamide and gave 60%, 50 % 43% yields respectively. These low yields were probably due to loss of catalyst's active sites during the reaction work-up.

### 3.3. Reaction conditions

Nitrile (10 mM), NiCl<sub>2</sub>.6H<sub>2</sub>O (0.2 mM) NaOCl (20 mL), NaOH (10 mL). Reaction time was 3 hours. Entry 2 without metal salts, (entries 3, 4 and 5 were carried out at 60°C and 80 °C and 100 °C respectively). Entries 6,7 and 8 recycling of NiO,

$$TO = \frac{\text{Moles of amide}}{\text{Moles of catalyst}}, \text{ TOF} = \frac{\text{Turnover}}{\text{Time (h)}}$$

The scope of these catalytic systems was also studied using different substrates. All results were displayed in Table 3. The substrate scope for this catalytic system, NiCl<sub>2</sub>.6H<sub>2</sub>O/NaOCl/NaOH was investigated by using different *p*-substituents. It was noticed that the substrates with para-substituted electron-deficient group like, *p*-Cl, *p*-NO<sub>2</sub> and *p*-CF<sub>3</sub> (entries 9,10 and 11, Table 3) gave higher yields than higher than the substrates with found with para-substituted electron-sufficient groups like, *p*-CH<sub>3</sub>, *p*-OH and *p*-NH<sub>2</sub> (entries 12, 13 and 14 Table 3). This confirmed that the electron-deficient groups enhanced the electrophilicity of carbon nitrile for the nucleophilic addition by two water molecules to form the corresponding amides (Ahmed *et al.*, 2011).

**Table 3:** The substrate scope the catalytic hydration of some *p*-substituted nitriles to amides.

20 mL NaOCl (5.25%), 10 ml NaOH (1.0 M)  
 0.2 mM of metal salt and 20 mM of nitrile

R = Cl, NO<sub>2</sub>, F<sub>3</sub>C, CH<sub>3</sub>, OH and NH<sub>2</sub>,

Entry	Substrate	Product	NiCl <sub>2</sub> .6H <sub>2</sub> O			CuCl <sub>2</sub> .6H <sub>2</sub> O			Fe(NO <sub>3</sub> ) <sub>3</sub> .9H <sub>2</sub> O		
			Y (%)	TO	TOF (h <sup>-1</sup> )	Y (%)	TO	TOF (h <sup>-1</sup> )	Y (%)	TO	TOF (h <sup>-1</sup> )
9			97	48.5	16.2	70	35	11.7	50	25	6.25
10			95	47.5	15.8	69	34.5	11.5	55	27	9.16
11			96	48	16	72	36	12	54	27	9
12			90	45	15	69	34.5	11.5	50	25	8.33
13			88	44	14.7	65	32.5	8.3	50	25	8.33
14			85	42.5	14.2	72	36	9	38	19	6.33

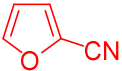
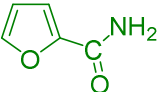
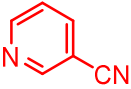
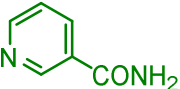
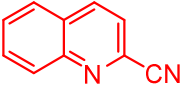
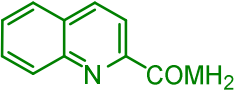
### 3.4. Reaction conditions

Nitrile (10 mM), metal salt (0.2 mM) NaOCl (20 mL), NaOH (10 mL). Reaction time was 3 hours,

$$TO = \frac{\text{Moles of amide}}{\text{Moles of catalyst}}, \quad TOF = \frac{\text{Turnover}}{\text{Time (h)}}$$

Three heterocyclic compounds, furan-2-carboxnitrile, pyridine-3-carbonitrile and quoline-2-carbonitrile were hydrated to furan-2-carboxamide, pyridine-3-carboxamide and quinoline-2-carboxamide respectively in good yields (entries 15, 16 and 17 Table 4).

**Table 4:** Catalytic hydration of some heterocyclic nitrile

Entry	Substrate	Product	NiCl <sub>2</sub> .6H <sub>2</sub> O			CuCl <sub>2</sub> .6H <sub>2</sub> O			Fe(NO <sub>3</sub> ) <sub>3</sub> .9H <sub>2</sub> O		
			Y (%)	TO	TOF (h <sup>-1</sup> )	Y (%)	TO	TOF (h <sup>-1</sup> )	Y (%)	TO	TOF (h <sup>-1</sup> )
15			94	47	15.66	70	35	11.16	60	30	10
16			95	47.5	15.83	65	32.5	10.83	45	22.5	7.5
17			96	48	16	68	34	0	45	22.5	7.5

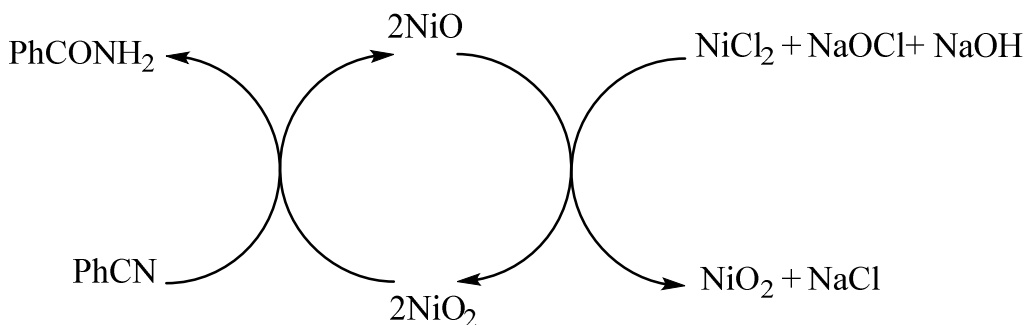
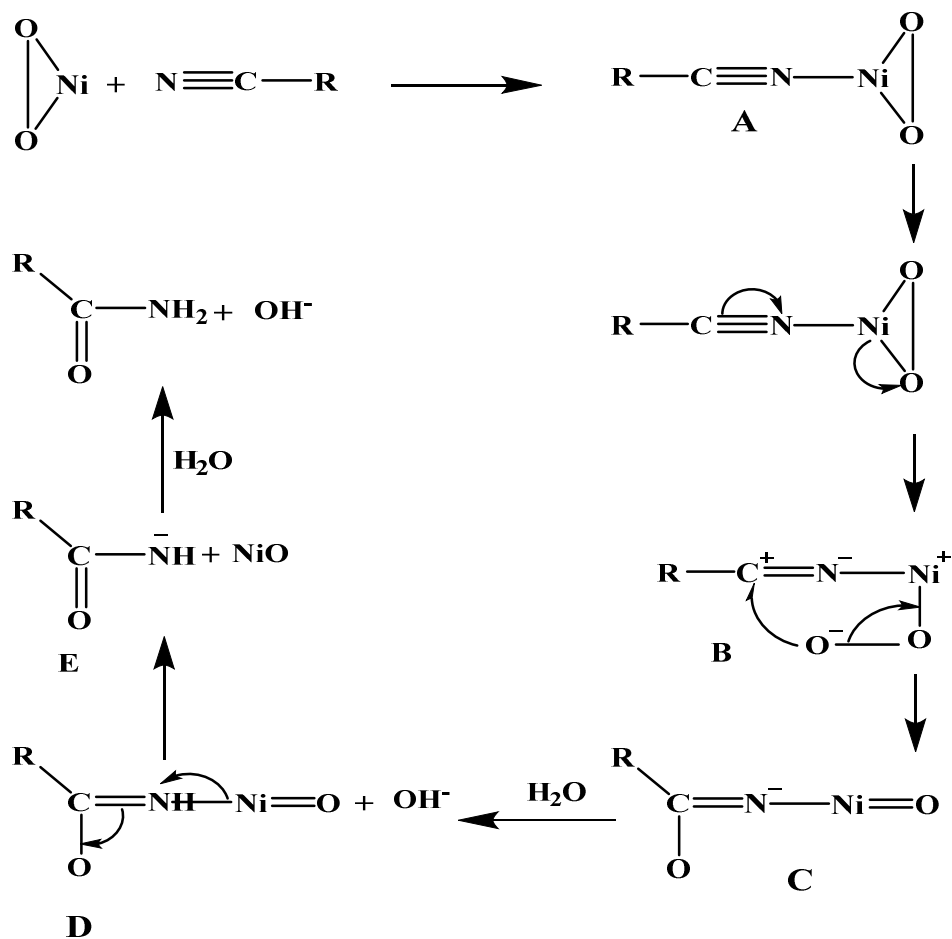
However, our results on these catalytic systems are comparable with some recently reported protocols (Duan and Song, 2024; Fan *et al.*, 2024, Procopio *et al.*, 2024).

Recently, Ma *et al* reported the synthesis of benzamide in water at 130 °C using the bimetallic catalyst Fe<sub>0.7</sub>Cu<sub>0.3</sub>O<sub>x</sub>-300 (Fan *et al.*, 2024). Gioia reported the synthesis of amide using the reactive deep eutectic solvents for amide synthesis ( Procopio *et al.*, 2024). Song *et al* reported the synthesis of amide by irradiation of oxamic acid and aryl bromide in the presence of organic photocatalyst, NiBr<sub>2</sub> and Na<sub>2</sub>CO<sub>3</sub> for 12 hours in dioxane as a solvent (Duan and Song, 2024). This protocol is superior to the above mentioned literatures in being works at room temperture, with shorter reaction and inexpensive chemicals. However, this reaction is green, selective (nitrile is hydrated to mainly to amide). Additionally, the solvent was water. Since the TOF is a measure of the catalytic activity of the catalyst ( Kozuch and Martin, 2012), It was found that the best yield and TOF were obtained with NiCl<sub>2</sub>.6H<sub>2</sub>O/NaOH/NaOCl (Entry 1, Table 1: TOF = 15.8), which means 15.8 mmole of benzamide will be formed per mole of NiCl<sub>2</sub>.6H<sub>2</sub>O per hour which in turn confirmed the periority of this catalyst system over the other two systems, CuCl<sub>2</sub>.6H<sub>2</sub>O and Fe(NO<sub>3</sub>)<sub>3</sub>.9H<sub>2</sub>O / NaOH/NaOCl.

### 3.5. Mechanism

The basic medium enhanced the electrophilicity of the nitrile carbon and the coordination of nitrile group to the Ni(II) center forming the complex (A). The reaction pathway in theory is mechanistically possible through the generation of the two aryl Ni(II) intermediates (B and C) Scheme 2.

The aryl nickel(II) complex (A) was thus underwent intermolecular rearrangement to produce aryl Ni(II)intermediates (B and C). The intermediate complex (C) was underwent electrophilic addition by water molecule to form the imido-Ni(II)oxo complex (D) which is unstable under these reaction conditions and intermolecularly dissociated to the imido anion (E) and NiO. The produced imido anion was further attacked by another one water molecule to for the corresponding amide The last two steps were promoted by the base (NaOH) present in the reaction medium, similar mechanism was suggested for the hydration of benzonitrile to benzamide by using NiCl<sub>2</sub>.6H<sub>2</sub>O and acetaldoxime in water as solvent (Cheung *et al.*, 2018 and Ma, *et al.*, 2012). During the progress of the reaction the grey-green color of NiO appeared with disappearance of black color of NiO<sub>2</sub>, this means the reaction is self-indicating. This catalytic cycle continued until the whole substrate was consumed, Scheme 3.



#### 4. Conclusion

The catalytic systems,  $\text{NiCl}_2 \cdot 6\text{H}_2\text{O}$ ,  $\text{CuCl}_2 \cdot 6\text{H}_2\text{O}$  and  $\text{Fe}(\text{NO}_3)_3 \cdot 9\text{H}_2\text{O} / \text{NaOH}/\text{NaOCl}$  have been prepared and used for the catalytic hydration of nitriles to their corresponding amides at room temperature. Key parameters, including yield (Y%), turnover (TO), and turnover frequency (TOF), were evaluated to determine the most Effective catalyst. The  $\text{NiCl}_2 \cdot 6\text{H}_2\text{O}/\text{NaOH}/\text{NaOCl}$  system showed the best results, with  $\text{NiO}_2$  identified as the active species for nitrile hydration. Characterization techniques revealed  $\text{NiO}_2$  spherical nanoparticles with average particle size of nm. Zeta potential is

equal to -3.98 mV indicating that the particles possess a negative surface charge. The surface texture study revealed that NiO<sub>2</sub> is mesoporous nanoparticle with high surface area ( $S_{\text{BET}}$ ) of 38.6 m<sup>2</sup>/g and average pore radius 2.77 nm. The highest yields of amides were achieved by the Ni-system. The mechanism proposed involves NiCl<sub>2</sub>·6H<sub>2</sub>O reacting with NaOCl to produce NiO<sub>2</sub>, which then reacts with the nitriles to form amides and NiO. The NiO can be recycled using excess NaOCl for further reactions.

### Acknowledgement

The author extend his appreciation to Taif university; Saudi Arabia for supporting this work through project number (TU-DSPP2024-95).

**Funding:** This work was funded by Taif University, Saudi Arabia, project number (TU-DSPP2024-95).

**Conflict of interest:** The author declares that there is no conflict of interest regarding the publication of this article".

**Availability of data and material:** The datasets generated and analyzed during the current study are available from the corresponding author.

### References

- Ahmed, T.J., S.M.M. Knapp, and D.R. Tyler, 2011. Frontiers in catalytic nitrile hydration: Nitrile and cyanohydrin hydration catalyzed by homogeneous organometallic complexes. *Coordination Chemistry Reviews*, 255(7-8): 949-974.
- Ali, I., et al., 2021. Experimental and simulation studies to determine the mechanisms of catalyst formation for the targeted synthesis of carbon nanotubes. *Journal of Nanoparticle Research*, 23: 1-11.
- Almada, N., 2023. Development of a PNN Pincer Ligand and Its Iron and Cobalt Complexes for Selective Catalytic Amide Synthesis, Middle Tennessee State University.
- Almalki, A.S., et al., 2022. Design, synthesis, anticancer activity and molecular docking studies of new benzimidazole derivatives bearing 1, 3, 4-oxadiazole moieties as potential thymidylate synthase inhibitors. *New Journal of Chemistry*, 46(31):14967-14978.
- Alsharif, M.A., et al., 2022. Divergent synthesis of fused Benzo-xanthene and oxazine derivatives via Cu-catalyst. *Journal of Saudi Chemical Society*, 26(6):101568.
- Ambalgi, S.M., et al., 2016. Synthesis, characterization and electrical properties of polyaniline/nickel oxide nanocomposites. *International Journal of Engineering Research*, 5(2): 119-122.
- Arai, H., et al., 2002. Structural and thermal characteristics of nickel dioxide derived from LiNiO<sub>2</sub>. *Journal of Solid State Chemistry*, 163(1): 340-349.
- Aziz, S.A., R.S. Ali, and A.N. Abd, 2020. Characterization studies of nickel oxide nanostructure films prepared by electrolysis method for photo detectors applications. *NeuroQuantology*, 18(2): 45.
- Cariati, E., et al., 2003. Efficient catalytic hydration of acetonitrile to acetamide using [Os (CO) 3Cl<sub>2</sub>] 2. *Journal of Molecular Catalysis A: Chemical*, 204: 279-285.
- Cheng, Z., et al., 2010. A facile and novel synthetic route to Ni (OH)<sub>2</sub> nanoflowers. *Superlattices and Microstructures*, 48(2): 154-161.
- Cheung, C.W., M.L. Ploeger, and X. Hu, 2018. Amide synthesis via nickel-catalysed reductive aminocarbonylation of aryl halides with nitroarenes. *Chemical science*, 9(3): 655-659.
- Chowdhury, S., et al., 2022. Decomposition of hydrogen peroxide using chemical and catalytic methods: A reactor-based approach. *Asian, J. Chem*, 34: 1263-1268.
- Comotti, M., et al., 2004. The catalytic activity of "naked" gold particles. *Angewandte Chemie International Edition*, 43(43): 5812-5815.
- Cychosz, K.A., et al., 2017. Recent advances in the textural characterization of hierarchically structured nanoporous materials. *Chemical Society Reviews*, 46(2): 389-414.
- de Figueiredo, R.M., J.-S. Suppo, and J.-M. Campagne, 2016. Nonclassical Routes for Amide Bond Formation. *Chemical Reviews*, 116(19):12029-12122.
- Dey, S. and N. Mehta, 2020. Oxidation of carbon monoxide over various nickel oxide catalysts in different conditions: A review. *Chemical Engineering Journal Advances*, 1: 100008.

- Djoman, M.C.K.-B. and A.N. Ajjou, 2000. The hydration of nitriles catalyzed by water-soluble rhodium complexes. *Tetrahedron Letters*, 41(25): 4845-4849.
- Duan, D. and L. Song, 2024. Photoredox Ni-catalyzed decarboxylative arylation of oxamic acids for amide synthesis. *Organic Chemistry Frontiers*, 11(1): 47-52.
- Fan, T., et al., 2024. Amorphous Fe<sub>0</sub>. 7Cu<sub>0</sub>. 3O<sub>x</sub> as a Bifunctional Catalyst for Selective Hydration of Nitriles to Amides in Water. *ACS Sustainable Chemistry & Engineering*, 12(20): 7791-7801.
- Feng, Y., et al., 2022. Synthesis and characterization of poly (butanediol sebacate-butanediol) terephthalate (PBSeT) reinforced by hydrogen bond containing amide group, with good mechanical properties and improved water vapor barrier. *Advanced Composites and Hybrid Materials*, 5(3): 2051-2065.
- Govindaraj, D., et al., 2024. Fumed Silica Support as a Catalytic Platform, Ni and Mn Oxide Reactive Species for the Selective Hydration of Aromatic Nitriles. *Silicon*, 16(2):853-866.
- Han, S. and J. Wu, 2022. Recent advances of poly (ester amide) s-based biomaterials. *Biomacromolecules*, 23(5):1892-1919.
- Hazarika, S. and G. Borah, 2023. Green synthesis of reduced graphene oxide anchored Fe<sub>3</sub>O<sub>4</sub>-Pd hetero-nanostructure: An efficient, magnetically separable and reusable catalyst for Beckmann rearrangement of aldoximes to amides. *Applied Organometallic Chemistry*, 37(12): e7275.
- Hu, D.Y., et al., 2008. Synthesis and antiviral activities of amide derivatives containing the  $\alpha$ -aminophosphonate moiety. *Journal of agricultural and food chemistry*, 56(3): 998-1001.
- Kabirb, S.F., et al., 2021. Effects of amide-based modifiers on surface activation and devulcanization of rubber. *Computational Materials Science*, 188: 110175.
- Kaminskaia, N., I. Guzei, and N. Kostić, 1998. Interplay between the palladium (II) ion, unidentate ligands and hydroxyl groups from a bidentate ligand in a new complex that catalyses hydration and alcoholysis of nitrile and urea. *Journal of the Chemical Society, Dalton Transactions*, 22: 3879-3886.
- Kopylovich, M.N., et al., 2002. Zinc (II)/ketoxime system as a simple and efficient catalyst for hydrolysis of organonitriles. *Inorganic Chemistry*, 41(18): 4798-4804.
- Kozuch, S. and J.M. Martin, 2012. "Turning over" definitions in catalytic cycles., ACS Publications, 2787-2794.
- Lu, Y., et al., 2024. Anodic electrosynthesis of amide from alcohol and ammonia. *CCS Chemistry*, 6(1): 125-136.
- Luo, H., et al., 2023. Metal-Free Nitrogen-Doped Porous Carbons for Nitriles and Amides Synthesis from 1, 2-Diols via Oxidative Cleavage of C–C Bonds. *ACS Catalysis*, 13(22): 14996-15006.
- Lutz-Röder, A., M. Jezussek, and P. Winterhalter, 1999. Nickel peroxide induced oxidation of canthaxanthin. *Journal of agricultural and food chemistry*, 47(5): 1887-1891.
- Ma, X., et al., 2012. The hydration of nitriles catalyzed by simple transition metal salt of the fourth period with the aid of acetaldoxime. *Applied Organometallic Chemistry*, 26(7): 377-382.
- Martin, M., et al., 2009. Water-soluble triisopropylphosphine complexes of ruthenium (II): synthesis, equilibria, and acetonitrile hydration. *Organometallics*, 28(2): 561-566.
- Massolo, E., M. Pirola, and M. Benaglia, 2020. Amide bond formation strategies: Latest advances on a dateless transformation. *European Journal of Organic Chemistry*, 30: 4641-4651.
- Montalbetti, C.A. and V. Falque, 2005. Amide bond formation and peptide coupling. *Tetrahedron*, 61(46): 10827-10852.
- Moradnia, F., et al., 2024. Green synthesis of nickel oxide nanoparticles using plant extracts: an overview of their antibacterial, catalytic, and photocatalytic efficiency in the degradation of organic pollutants. *Iranian Journal of Catalysis (IJC)*, 14(1): 1-24.
- Nakagawa, K. and T. Tsuji, 1963. Oxidation with Nickel Peroxide. II. Oxidation of Amines. *Chemical and Pharmaceutical Bulletin*, 11(3): 296-301.
- Nakagawa, K., et al., 1979. Oxidation with nickel peroxide. XII. Synthesis of nitriles from aldehydes. *Synthetic Communications*, 9(6):529-534.
- Nakagawa, K., H. Onoue, and J. Sugita, 1964. Oxidation with nickel peroxide. iv. The preparation of benzoxazoles from Schiff's bases. *Chemical and Pharmaceutical Bulletin*, 12(10):1135-1138.
- Nakagawa, K., H. Onoue, and K. Minami, 1966. Oxidation with nickel peroxide. A new synthesis of amides from aldehydes or alcohols. *Chemical Communications (London)*, 1: 17-18.

- Nakagawa, K., R. Konaka, and T. Nakata, 1962. Oxidation with nickel peroxide. I. Oxidation of alcohols. *The Journal of Organic Chemistry*, 27(5): 1597-1601.
- Ogoshi, S., 2020. Nickel catalysis in organic synthesis: methods and reactions.
- Pattabiraman, V.R. and J.W. Bode, 2011. Rethinking amide bond synthesis. *Nature*, 480(7378): 471-479.
- Procopio, D., C. Siciliano, and M.L. Di Gioia, 2024. Reactive deep eutectic solvents for EDC-mediated amide synthesis. *Organic & Biomolecular Chemistry*, 22(7): 1400-1408.
- Qiao, H., et al., 2009. Preparation and characterization of NiO nanoparticles by anodic arc plasma method. *Journal of Nanomaterials*, 1-5.
- Rehman, W.U., et al., 2023. Co<sub>3</sub>O<sub>4</sub>/NiO nanocomposite as a thermocatalytic and photocatalytic material for the degradation of malachite green dye. *Journal of Materials Science: Materials in Electronics*, 34(1): 15.
- Shoair, A.G.F., et al., 2023. Unlocking the Potential of NiSO<sub>4</sub>·6H<sub>2</sub>O/NaOCl/NaOH Catalytic System: Insights into Nickel Peroxide as an Intermediate for Benzonitrile Synthesis in Water. *Journal of Nanotechnology*, 1: 9940845.
- Singh, H., et al., 2019. Nanoporous nickel oxide catalyst with uniform Ni dispersion for enhanced hydrogen production from organic waste. *International Journal of Hydrogen Energy*, 44(36): 19573-19584.
- Sirtes, G., et al., 2005. The effects of temperature on sodium hypochlorite short-term stability, pulp dissolution capacity, and antimicrobial efficacy. *Journal of endodontics*, 31(9): 669-671.
- Sreenavya, A., F. Muhammed, and A. Sakthivel, 2021. Porous nickel oxide derived from Ni (OH)<sub>2</sub>: preparation, characterization, and catalytic applications. *Emergent Materials*, 4: 803-809.
- Tilvez, E., M.I. Menendez, and R. Lopez, 2013. Unraveling the reaction mechanism on nitrile hydration catalyzed by [Pd (OH)<sub>2</sub> 4]<sup>2+</sup>: insights from theory. *Inorganic chemistry*, 52(13): 7541-7549.
- van der Waal, S.V., N.E. van Dusseldorp, and J.J. de Soet, 2014. An evaluation of the accuracy of labeling of percent sodium hypochlorite on various commercial and professional sources: is sodium hypochlorite from these sources equally suitable for endodontic irrigation? *Journal of endodontics*, 40(12): 2049-2052.
- Vyas, K.M., et al., 2020. Arene-ruthenium (II)-phosphine complexes: Green catalysts for hydration of nitriles under mild conditions. *Inorganic Chemistry Communications*, 112: 107698.
- Wang, H., et al., 2019. Nanorod manganese oxide as an efficient heterogeneous catalyst for hydration of nitriles into amides. *Industrial & Engineering Chemistry Research*, 58(37): 17319-17324.
- Waqas, M., et al., 2020. Support effect on the catalytic activity and stability of non-crystal ternary oxides. *Colloids and Surfaces A: Physicochemical and Engineering Aspects*, 586: 124218.
- Wei, Z., et al., 2009. Characterization of NiO nanoparticles by anodic arc plasma method. *Journal of alloys and compounds*, 479(1-2):855-858.
- Wu, W., et al., 2022. Safe and stable lithium metal batteries enabled by an amide-based electrolyte. *Nano-Micro Letters*, 14(1):44.
- Yang, L.-X., et al., 2007. Hydrothermal synthesis of nickel hydroxide nanostructures in mixed solvents of water and alcohol. *Journal of Solid State Chemistry*, 180(7): 2095-2101.